AJNR

This information is current as of August 19, 2025.

Association of Isolated Congenital Heart Disease with Fetal Brain Maturation

C. Jaimes, V. Rofeberg, C. Stopp, C.M. Ortinau, A. Gholipour, K.G. Friedman, W. Tworetzky, J. Estroff, J.W. Newburger, D. Wypij, S.K. Warfield, E. Yang and C.K. Rollins

Association of Isolated Congenital Heart Disease with Fetal Brain Maturation

C. Jaimes, V. Rofeberg, C. Stopp, C.M. Ortinau, A. Gholipour, K.G. Friedman, W. Tworetzky, J. Estroff, J.W. Newburger, D. Wypij, S.K. Warfield, E. Yang, and C.K. Rollins

ABSTRACT

BACKGROUND AND PURPOSE: Brain MRI of newborns with congenital heart disease show signs of immaturity relative to healthy controls. Our aim was to determine whether the semiquantitative fetal total maturation score can detect abnormalities in brain maturation in fetuses with congenital heart disease in the second and third trimesters.

MATERIALS AND METHODS: We analyzed data from a prospective study of fetuses with and without congenital heart disease who underwent fetal MR imaging at 25–35 weeks' gestation. Two independent neuroradiologists blinded to the clinical data reviewed and scored all images using the fetal total maturation score. Interrater reliability was evaluated by the intraclass correlation coefficient using the individual reader scores, which were also used to calculate an average score for each subject. Comparisons of the average and individual reader scores between affected and control fetuses and relationships with clinical variables were evaluated using multivariable linear regression.

RESULTS: Data from 69 subjects (48 cardiac, 21 controls) were included. High concordance was observed between readers with an intraclass correlation coefficient of 0.98 (95% CI, 0.97–0.99). The affected group had significantly lower fetal total maturation scores than the control group (β-estimate, –0.9 [95% CI, –1.5 to –0.4], $P = .002$), adjusting for gestational age and sex. Averaged fetal total maturation, germinal matrix, myelination, and superior temporal sulcus scores were significantly delayed in fetuses with congenital heart disease versus controls ($P < .05$ for each). The fetal total maturation score was not significantly associated with any cardiac, anatomic, or physiologic variables.

CONCLUSIONS: The fetal total maturation score is sensitive to differences in brain maturation between fetuses with isolated congenital heart disease and healthy controls.

ABBREVIATIONS: CHD = congenital heart disease; fTMS = fetal total maturation score; fTMSav = averaged fetal total maturation score; fTMSi = individual fetal total maturation score; GA = gestational age

Congenital heart disease (CHD) is the most common congenital anomaly, affecting approximately 8 neonates per 1000 live births.[1] Survivors are at increased risk of cerebral white matter injury and adverse neurodevelopmental outcomes including developmental delay, lower academic achievement, compromised motor function, and learning disabilities.[2-5] These adverse outcomes have prompted investigations of brain development in patients with CHD, particularly with the use of noninvasive imaging techniques. Several studies have documented abnormalities in the brains of neonates with CHD before surgical intervention. These abnormalities include both smaller brain volumes and dysmaturation as measured by diffusion-weighted imaging,

MR spectroscopy, and the semiquantitative multiparametric postnatal total maturation score.[6-8] A combination of altered cerebral perfusion, compromised substrate delivery, and abnormal gene expression is likely to contribute to these findings.[2,9]

The presence of neuroimaging abnormalities in preoperative neonates suggests a prenatal onset. An accelerated rate of brain growth coupled with elevated metabolic demands and a highly regulated pattern of gene expression render the brain particularly vulnerable during the second and third trimesters.[10,11] For example, during the second half of gestation, the brain more than doubles in size and neuronal progenitors migrate toward their cortical targets.[12-14] Gyrification also advances rapidly, with the emergence of the primary sulci between 18 and 32 weeks.[15,16] Myelination of the brain stem and deep gray nuclei becomes apparent on MR imaging.[17,18] Last, as mitotic activity in the ventricular and subventricular zone declines, the germinal matrix starts to involute.[14] Prior studies support a prenatal vulnerability by demonstrating decreased brain volumes, a reduced gyrification index, abnormal metabolic ratios on MR spectroscopy, and an increased apparent diffusion coefficient in fetuses with CHD.[19-22] While these findings provide valuable insights into pathophysiology, they rely on computational analysis techniques and/or sequences that are not routinely available in a clinical setting.

Recently, Vossough et al[23] introduced and validated a semiquantitative multiparametric fetal total maturation score (fTMS), an extension of the postnatal total maturation score, which can be readily calculated using routine, clinically acquired fetal brain MR imaging. The fTMS evaluates gyrification/sulcation, the presence of the germinal matrix, and myelination in utero. Postnatal total maturation scores were previously found to differ between CHD and control neonates.[24] We applied the fTMS to fetuses with and without CHD to investigate whether maturational differences could be detected in utero in the CHD population compared with a control group.

MATERIALS AND METHODS
This study analyzed a subset of data from an institutional review board–approved Health Insurance Portability and Accountability Act–compliant prospective, longitudinal cohort study comparing brain development in fetuses with CHD with that in healthy controls (Boston Children's Hospital, Boston, MA). Patients included in this analysis were recruited between February 2014 and May 2017. Written informed consent was obtained from all pregnant women. Inclusion criteria for the overall cohort of fetuses with CHD were the following: nontrivial CHD confirmed by fetal echocardiogram, maternal age of 18–45 years, and gestational age (GA) of 18–30 weeks at the time of recruitment. Exclusion criteria included multiple-gestation pregnancy, maternal CHD, the presence of a noncardiac fetal anomaly, a known genetic abnormality, congenital infection, contraindications to MR imaging, or referring clinician deemed recruitment inappropriate (eg, family distress, considering termination). Control subjects were recruited from a pool of patients who underwent a screening fetal echocardiogram due to a family history of CHD but had no detected cardiac, genetic, or other organ abnormality. Control subjects were selected to approximately match the sex and GA at MR imaging of the CHD cohort. In the overarching longitudinal study, subjects underwent 2 fetal MRIs, the first at 18–30 weeks' gestation and the second at 36–40 weeks' gestation. In some cases, fetuses were imaged outside of the target window for scheduling reasons. Because the fTMS was designed to assess brain maturation at 25–35 weeks' gestation, for the present analysis, subjects with MRIs performed in this GA range were included. If a given subject had 2 MRIs between 25 and 35 weeks' gestation, only the earlier MR imaging was analyzed. If the super-resolution reconstruction used for analysis (see below) was of poor quality, the subject was excluded.

We recorded maternal demographic information and fetal clinical data for all subjects. Maternal data included race, ethnicity, age, and education at the time of delivery; fetal data included sex and GA at time of the MR imaging. For fetuses with CHD, we recorded the diagnosis on the basis of a fetal echocardiogram, which was later confirmed with postnatal echocardiography. Anatomic and physiologic variables were also recorded from the fetal echocardiogram and included ventricular physiology (2 ventricle versus single ventricle), the presence versus absence of aortic arch hypoplasia, antegrade-versus-retrograde aortic arch flow, and combined systemic and pulmonary cardiac output. All fetal echocardiograms were obtained as part of routine clinical care, and their values were reviewed by an experienced cardiologist with expertise in fetal echocardiography.

Image Acquisition and Processing
Subjects were scanned on a 3T MR imaging system (Magnetom Skyra; Siemens) using an 18-channel body array coil. Multiplanar single-shot fast spin-echo T2-weighted sequences were acquired in multiple planes with 2 interleaves and with a TR of 1.4–2 seconds, a TE of 120 ms, a section thickness of 2–3 mm, and no interslice gap. At least 3 sets of single-shot fast spin-echo T2-weighted images were acquired in each plane, with FOVs of 256 × 256 or 320 × 320. The multiplanar single-shot fast spin-echo images were processed using a previously validated fetal MR imaging processing pipeline,[25] which involved a section-to-volume reconstruction algorithm[26] that generated motion-corrected, intensity-normalized, super-resolution 3D volumes with 0.75-mm isotropic voxels in the scanner (world) coordinates and registration to a normative spatiotemporal MR imaging atlas of the fetal brain for review in standard anatomic planes. The reconstructed images were thus reviewed in standard anatomic planes to minimize variations in scoring due to slight differences in the orientation of the fetus or the position of the mother.

Image Analysis
The fTMS was used to assess brain maturation for each subject. Ordinal values were assigned to several features including gyrification of the frontal and occipital lobes (1–4), gyrification of the insula (1–3), presence of the superior temporal sulcus (0–2), presence of the inferior temporal sulcus (0–2), germinal matrix involution (1–3), and stage of myelination (1–3) to create subscores for each of these components of brain maturation. As described by Vossough et al,[23] each feature was scored separately for each hemisphere. The results were then averaged to produce a single subscore for each feature, and the subscores were summed to create the fTMS for each subject. Images were reviewed and scored independently by 2 neuroradiologists with 8 and 2

Table 1: Maternal and fetal characteristics

Variables	All (*n* = 69)	CHD (*n* = 48)	Controls (*n* = 21)	P Value[a]
Maternal characteristics				
Race (No.) (%)				>.99
Black	2 (3)	2 (4)	0	
White	64 (93)	44 (92)	20 (95)	
Other	3 (4)	2 (4)	1 (5)	
Hispanic ethnicity (No.) (%)	9 (13)	6 (13)	3 (14)	>.99
Education, bachelor's degree or higher (No.) (%)	34 (51)	23 (50)	11 (52)	>.99
Estimated age at delivery (median) (range) (yr)	31.6 (18.7–40.4)	31.8 (18.7–40.4)	30.0 (23.0–37.5)	.68
Fetal characteristics				
Male sex, n (%)	38 (55)	28 (58)	10 (48)	.44
Gestational age at MR imaging (median) (range) (yr)	28.3 (25.1–33.3)	29.4 (25.9–33.3)	26.9 (25.1–33.1)	.003

[a] P values for group comparisons were determined by Fisher exact tests for categoric variables and Wilcoxon rank sum tests for continuous variables.

years of experience to produce individual fTMS values (fTMSi values) for each subject, which were subsequently averaged to generate the averaged fTMS (fTMSav). Before scoring the data for research purposes, the 2 readers jointly reviewed a set of 15 random cases to set standards for interpretation. The scoring of the subjects occurred 1 month after standards were set, to avoid recall bias.

Statistical Analysis

Fisher exact tests and Wilcoxon rank sum tests were used to compare maternal and fetal characteristics between the CHD and control groups. Interrater reliability was assessed with the intraclass correlation coefficient. Multivariable linear regression was used to evaluate the effect of group (CHD versus control), GA, and sex on the fTMSav and each fTMSi, with ordinal logistic regression used in follow-up analyses of the same effects on each subscore. Linear regression was also used to evaluate the effect of echocardiographic variables on fTMSav. Delays in brain maturation were estimated using a grid search with steps of 0.01 weeks' gestational age for the fTMSav as well as each subscore, using linear and ordinal logistic regression, respectively, without adjustment for sex. $P < .05$ was considered statistically significant.

RESULTS

Sample

From a total of 107 prospectively recruited pregnant women, 75 had MRIs performed at 25–35 weeks' gestation. We excluded 6 subjects due to poor image quality related to excessive motion or artifacts. Therefore, data from 69 subjects (48 with CHD, 21 controls) were used in our analysis. Each subject contributed 1 MR imaging during the target GA range. Table 1 summarizes maternal and fetal characteristics.

Fetal Echocardiography

Anatomic evaluation of the fetuses with CHD revealed that 9 (19%) had hypoplastic left-heart syndrome, 4 (8%) had fetal aortic stenosis, 5 (10%) had tetralogy of Fallot, 5 (10%) had transposition of the great arteries, 11 (23%) had other single-ventricle CHD, and 14 (29%) had other 2-ventricle CHD.

Regarding the physiology of the fetuses with CHD, 22 (46%) had single-ventricle physiology, 26 (54%) had aortic arch hypoplasia, and 33 (68%) had antegrade aortic flow. The median
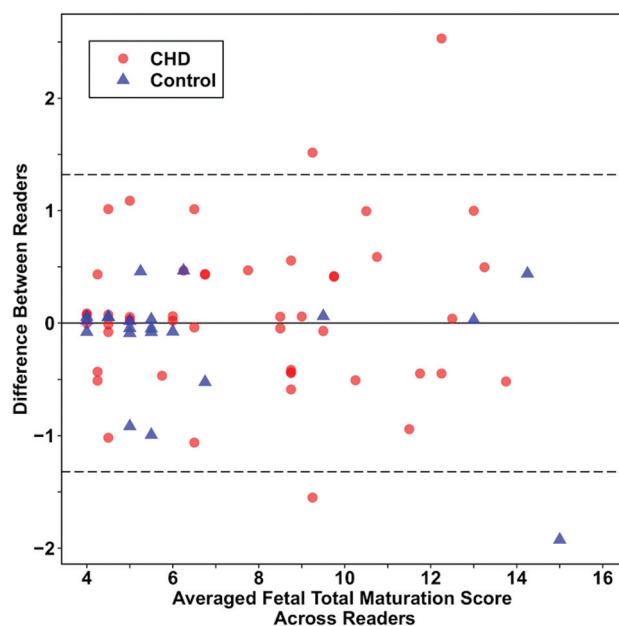

FIG 1. Bland-Altman plot demonstrating high interrater reliability. The overall mean difference between readers was 0.01 (95% CI, 0.14–0.17).

combined cardiac output was 0.45 L/min/Kg (range, 0.17–0.77 L/min/Kg) for fetuses with CHD and 0.43 (range, 0.19–0.90 L/min/Kg) for control fetuses. There were no statistically significant differences in combined cardiac output between groups (Wilcoxon rank sum, $P = .91$).

CHD and Brain Maturation

Excellent interrater agreement was observed for the fTMS values with an intraclass correlation coefficient of 0.98 (95% CI, 0.97–0.99). For the CHD group and control group, the intraclass correlation coefficients were 0.97 (95% CI, 0.96–0.99) and 0.99 (95% CI, 0.97–0.998), respectively. A Bland-Altman plot (Fig 1) showed a mean difference between readers of 0.01 (95% CI, –0.14–0.17).

The CHD group had a lower fTMSav than the control group (β-estimate, –0.9 [95% CI, –1.5 to –0.4], $P = .002$) after adjusting for GA and sex (Figs 2 and 3). A similar group difference was observed for each fTMSi ($P < .01$ for each). Significant relationships of fTMSav with GA (β-estimate, 1.4 [95% CI, 1.3–1.6] per week, $P < .001$) and each fTMSi with GA ($P < .001$ for each) were also
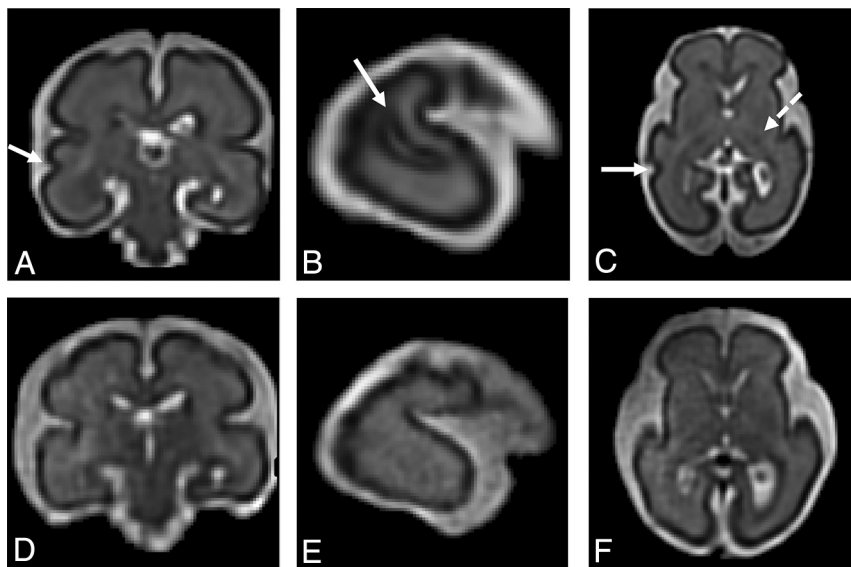
FIG 2. Differences in fTMS values between a control subject and a fetus in the second trimester. A–C, Multiplanar reformatted images from a 26-week 6-day-old control fetus with an fTMS of 6.5 shows early development of the right superior temporal sulcus (A, B, and C; *arrow*) and early myelination in the thalamus and posterior limb of the internal capsule (C, *dotted arrow*). D–F, Multiplanar reformatted images from a 26-week 6-day-old fetus with hypoplastic left-heart syndrome with an fTMS of 4 show a smooth temporal lobe (absent superior temporal sulcus) and lack of myelination.
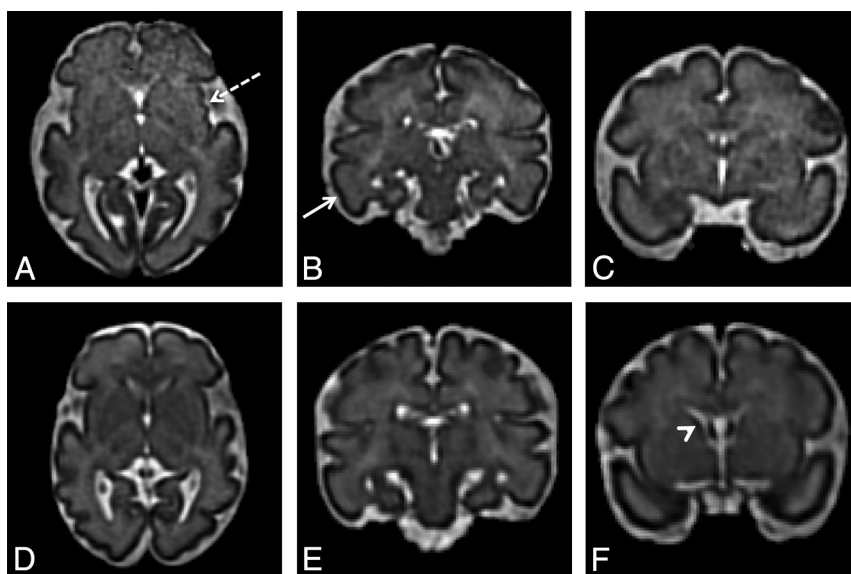
FIG 3. Differences in fTMS between a control subject and a subject with CHD in the third trimester. A–C, Multiplanar reformatted images from a 30-week 6-day-old control fetus with an fTMSav of 14 show early insular sulcation (A, *dotted arrow*), a developing inferior temporal sulcus (B, *solid arrow*), and no residual germinal matrix (C). D–F, Multiplanar reformatted images from a 31-week 2-day old fetus with tricuspid atresia and an fTMS of 10 show a smooth insula (D), no evidence of a developing inferior temporal sulcus (E), and some residual germinal matrix (F, *arrowhead*).

observed after adjusting for group and sex. Linear relationships of fTMSav with GA in fetuses with CHD and controls ($R^2 = 0.86$ and $R^2 = 0.92$, respectively) were noted (Fig 4). No effect of sex on fTMSav (β-estimate, 0.3 [95% CI, –0.2–0.8], $P = .25$) or either fTMSi ($P > .10$ for each) was observed. Parameter estimates for the individual readers are available in the On-line Table.

Significant delay was observed for the fTMSav (β-estimate, 0.7 weeks [95% CI, 0.3–1.0], $P = .001$) and the germinal matrix (β-estimate, 2.0 [95% CI, 1.2–2.7], $P < .001$), myelination (β-estimate, 1.1 [95% CI, 0.2–1.9], $P = .02$), and superior temporal sulcus (β-estimate, 0.9 [95% CI, 0.3–1.4], $P = .002$) subscores (Fig 5). Estimated delays for all scores are summarized in Table 2.

Effect of Echocardiographic Variables on FTMS

In the CHD group, no statistically significant associations of fTMSav with any of the echocardiographic variables were observed after adjusting for GA and sex (Table 3).
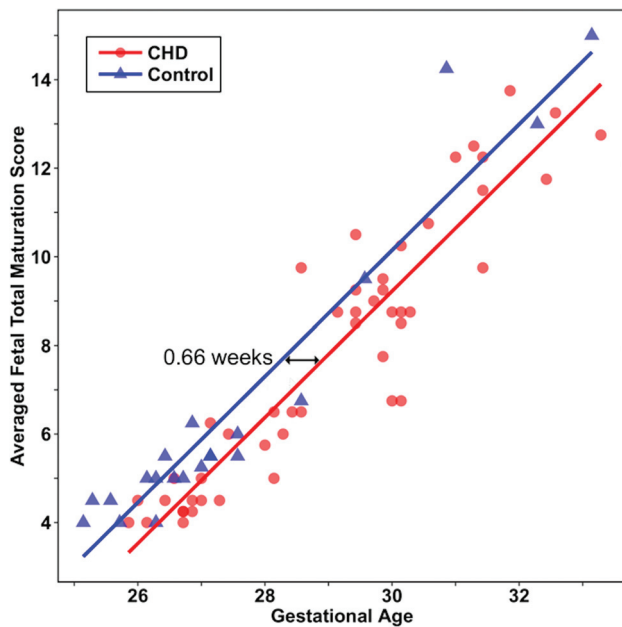
DISCUSSION

We compared brain maturation between fetuses with and without CHD using the previously validated fTMS and documented that this semiquantitative score is sensitive to delays in brain maturation that are present during the second and early third trimester in fetuses with CHD. These results are consistent with prior reports of quantitative abnormalities in brain maturation of fetuses with CHD that have been described using MR spectroscopy, global parenchymal volumetry, and metrics of cortical development.[19-21]
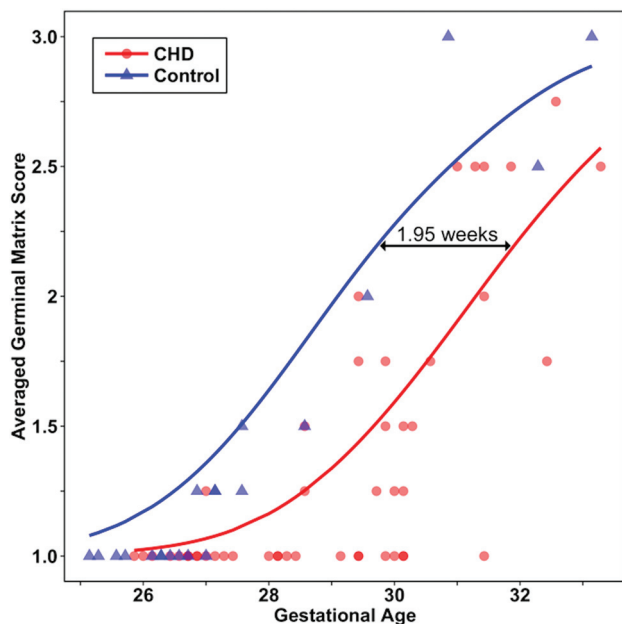
The main advantage of the fTMS is that it can be used in a routine clinical environment. The score is highly reproducible and has high interrater reliability,[23] which we independently verified for the first time in this work. Our results also expand previous work by validating the use of fTMS for data acquired at 3T, which is increasingly used in clinical practice.[27] Moreover, our observations approximate those of Vossough et al,[23] by confirming a linear relationship between fTMS and GA and suggest that the fTMS is feasible for clinical implementation.

The fTMS showed an overall brain maturational delay of approximately 1-week gestation in the subjects with CHD relative to controls, which highlights the prenatal onset of abnormalities in brain development in CHD. Our results differ from the approximate 4-week delay reported on postnatal total maturation score of neonates with CHD.[24] In part, this discrepancy may be due to differences in postconceptional age at the

FIG 4. Scatterplot illustrating the estimated delay in fTMSav values in fetuses with CHD compared with controls. *Lines* are predicted fTMSav scores modeled by linear regression.

FIG 5. Scatterplot illustrating the estimated delay in averaged germinal matrix subscores in fetuses with CHD compared with controls. *Lines* are predicted averaged germinal matrix scores modeled by ordinal logistic regression.

Table 2: Estimated maturational delay in gestational age based on differences in scores between CHD and control groups

Variables	Estimated Delay (wks)	95% CI
fTMSav	0.7	0.3–1.0
Germinal matrix	2.0	1.2–2.7
Myelination	1.1	0.2–1.9
Superior temporal sulcus	0.9	0.3–1.4
Inferior temporal sulcus	0.4	−0.8–1.6
Fronto-occipital gyrification	0.1	−0.6–0.7
Insular gyrification	−0.8	−2.9–0.8

.

nontrivial CHD, some of which may have a lesser effect on brain maturation.[24]

Individual analyses of the subscores showed significant between-group differences for the germinal matrix, myelination, and superior temporal sulcus subscores. Delayed involution of the germinal matrix is consistent with prior observations from Licht et al,[24] who described persistence of the germinal matrix beyond term as well as a greater number and size of migrating glial bands in neonates with CHD relative to controls. Early myelinating structures (eg, dorsal brain stem, the ventrolateral thalami, and the posterior limb of the internal capsule) are highly active metabolically in the second half of gestation and the early neonatal period.[29,30] It is, therefore, conceivable that their high metabolic demands render them uniquely vulnerable to a decreased supply of substrates, which, in turn, may result in a delay in normal myelination in fetuses with CHD. The delay in the emergence of the superior temporal sulcus is consistent with a prior description of abnormalities in sulcation in the temporal lobe in fetuses with hypoplastic left heart syndrome reported by Clouchoux et al,[20] and in early emerging sulci (including the superior temporal sulcus) reported by Ortinau et al.[28] Although we did not find significant differences in the subscores for emerging sulcation in other regions evaluated in the fTMS, in 2 of the 3 remaining subscores, the direction of the findings was toward a delay in the CHD group. It is possible that we did not observe these differences due to the small sample size, heterogeneous CHD selection bias noted above, or greater sensitivity of quantitative computational neuroimaging techniques.[20,28] The precise cause of the abnormal gyrification is unclear; it likely reflects a complex interaction between altered hemodynamics and decreased substrate delivery, the impact of these variables on the genetic program that governs gyrification, or a genetic variant irrespective of hemodynamics.[31,32] The cause for the nonsignificant trend toward accelerated sulcation in the insula is unclear and could reflect random variance in the sample.

A limitation of our study is the heterogeneity of our sample. While we observed a group effect of CHDs on fTMSav and fTMSi for both readers, we did not find significant associations between the specific hemodynamic parameters derived from the fetal echocardiogram and the fTMS. It is possible that either using a homogeneous group or using a larger sample size, allowing for subgroup analysis, could detect individual associations within CHD diagnostic categories. Another limitation is that the control fetuses were younger than the fetuses with CHD, with most control fetuses younger than 28 weeks. While a larger sample of third trimester control fetuses would be desirable to better characterize the trends after 28 weeks, this discrepancy is unlikely to affect our

time of the analysis, with our subjects' mean GA being approximately 27 weeks and those analyzed by Licht et al[24] being imaged postnatally at term. The differences could also reflect a longitudinal progression of the delay in maturation, as reported by Ortinau et al.[28] Finally, selection bias could also play a role. The cohort of Licht et al included only neonates with severe forms of CHD (ie, hypoplastic left-heart syndrome and transposition of the great arteries), whereas our cohort included various forms of

Table 3: Effect of echocardiographic variables on fTMSav values in the CHD group

Variables	β-Estimate	95% CI	P Value[a]
Two-ventricle physiology (vs single ventricle)	0.30	−0.34–0.96	.34
Aortic arch hypoplasia (vs none)	0.40	−0.22–1.05	.19
Antegrade aortic flow (vs retrograde)	−0.04	−0.72–0.64	.91
Combined cardiac output (L/min/Kg)	1.8	−1.1–4.6	.22

[a] P values are adjusted for gestational age and sex, as determined by linear regression. Separate models were run to assess the effect of each echocardiographic variable on fTMSav.

overall observation of lower fTMS in CHD, given that maturational differences are known to exist postnatally and may accentuate in late gestation and perinatal periods.[28]

Another limitation is the uncertain clinical significance of our observations. Future studies are needed to examine the associations between the fTMS and neurodevelopmental outcome. Finally, caution should be exercised when comparing fTMSs from other data with the results from our study. The super-resolution reconstructions are uniformly oriented in standard planes, which may facilitate image analysis by reducing the obliquity of native acquisitions. Also, the spatial resolution of these reconstructions is higher than that of standard acquisitions, which could have an effect on gyrification subscores. However, we expect that group differences would remain, given that all of our data were acquired and processed in the same way.

CONCLUSIONS

Emerging abnormalities in brain development of fetuses with CHD can be detected using the fTMS in the late second and early third trimester. Additional work is needed to relate these findings to neurodevelopmental outcome and elucidate the clinical significance of these findings.

REFERENCES

1. Marelli AJ, Ionescu-Ittu R, Mackie AS, et al. **Lifetime prevalence of congenital heart disease in the general population from 2000 to 2010.** *Circulation* 2014;130:749–56 CrossRef Medline
2. Marelli A, Miller SP, Marino BS, et al. **Brain in congenital heart disease across the lifespan: the cumulative burden of injury.** *Circulation* 2016;133:1951–62 CrossRef Medline
3. Bellinger DC, Wypij D, Rivkin MJ, et al. **Adolescents with d-transposition of the great arteries corrected with the arterial switch procedure: neuropsychological assessment and structural brain imaging.** *Circulation* 2011;124:1361–69 CrossRef Medline
4. Bellinger DC, Wypij D, du Plessis AJ, et al. **Neurodevelopmental status at eight years in children with dextro-transposition of the great arteries: the Boston Circulatory Arrest Trial.** *J Thorac Cardiovasc Surg* 2003;126:1385–96 CrossRef Medline
5. Limperopoulos C, Majnemer A, Shevell MI, et al. **Predictors of developmental disabilities after open heart surgery in young children with congenital heart defects.** *J Pediatr* 2002;141:51–58 CrossRef Medline
6. Owen M, Shevell M, Donofrio M, et al. **Brain volume and neurobehavior in newborns with complex congenital heart defects.** *J Pediatr* 2014;164:1121–27.e1121 CrossRef Medline
7. Miller SP, McQuillen PS, Hamrick S, et al. **Abnormal brain development in newborns with congenital heart disease.** *N Engl J Med* 2007;357:1928–38 CrossRef Medline
8. Jaimes C, Cheng HH, Soul J, et al. **Probabilistic tractography-based thalamic parcellation in healthy newborns and newborns with congenital heart disease.** *J Magn Reson Imaging* 2018;47:1626–37 CrossRef Medline
9. Homsy J, Zaidi S, Shen Y, et al. **De novo mutations in congenital heart disease with neurodevelopmental and other congenital anomalies.** *Science* 2015;350:1262–66 CrossRef Medline
10. Smart JL, Dobbing J, Adlard BP, et al. **Vulnerability of developing brain: relative effects of growth restriction during the fetal and suckling periods on behavior and brain composition of adult rats.** *J Nutr* 1973;103:1327–38 CrossRef Medline
11. Miller JA, Ding SL, Sunkin SM, et al. **Transcriptional landscape of the prenatal human brain.** *Nature* 2014;508:199–206 CrossRef Medline
12. Clouchoux C, Guizard N, Evans AC, et al. **Normative fetal brain growth by quantitative in vivo magnetic resonance imaging.** *Am J Obstet Gynecol* 2012;206:e171–78 CrossRef Medline
13. Kolasinski J, Takahashi E, Stevens AA, et al. **Radial and tangential neuronal migration pathways in the human fetal brain: anatomically distinct patterns of diffusion MRI coherence.** *Neuroimage* 2013;79:412–22 CrossRef Medline
14. Chong BW, Babcook CJ, Salamat MS, et al. **A magnetic resonance template for normal neuronal migration in the fetus.** *Neurosurgery* 1996;39:110–16 CrossRef Medline
15. Garel C, Chantrel E, Brisse H, et al. **Fetal cerebral cortex: normal gestational landmarks identified using prenatal MR imaging.** *AJNR Am J Neuroradiol* 2001;22:184–89 Medline
16. Zhang Z, Hou Z, Lin X, et al. **Development of the fetal cerebral cortex in the second trimester: assessment with 7T postmortem MR imaging.** *AJNR Am J Neuroradiol* 2013;34:1462–67 CrossRef Medline
17. Counsell SJ, Maalouf EF, Fletcher AM, et al. **MR imaging assessment of myelination in the very preterm brain.** *AJNR Am J Neuroradiol* 2002;23:872–81 Medline
18. Kinney HC, Karthigasan J, Borenshteyn NI, et al. **Myelination in the developing human brain: biochemical correlates.** *Neurochem Res* 1994;19:983–96 CrossRef Medline
19. Limperopoulos C, Tworetzky W, McElhinney DB, et al. **Brain volume and metabolism in fetuses with congenital heart disease: evaluation with quantitative magnetic resonance imaging and spectroscopy.** *Circulation* 2010;121:26–33 CrossRef Medline
20. Clouchoux C, Du Plessis AJ, Bouyssi-Kobar M, et al. **Delayed cortical development in fetuses with complex congenital heart disease.** *Cereb Cortex* 2013;23:2932–43 CrossRef Medline
21. Berman JI, Hamrick SE, McQuillen PS, et al. **Diffusion-weighted imaging in fetuses with severe congenital heart defects.** *AJNR Am J Neuroradiol* 2011;32:E21–22 CrossRef Medline

22. Schellen C, Ernst S, Gruber GM, et al. **Fetal MRI detects early alterations of brain development in tetralogy of Fallot.** *Am J Obstet Gynecol* 2015;213:e391–97 CrossRef Medline

23. Vossough A, Limperopoulos C, Putt ME, et al. **Development and validation of a semiquantitative brain maturation score on fetal MR images: initial results.** *Radiology* 2013;268:200–07 CrossRef Medline

24. Licht DJ, Shera DM, Clancy RR, et al. **Brain maturation is delayed in infants with complex congenital heart defects.** *J Thorac Cardiovasc Surg* 2009;137:529–36; discussion 536–37 CrossRef Medline

25. Gholipour A, Rollins CK, Velasco-Annis C, et al. **A normative spatiotemporal MRI atlas of the fetal brain for automatic segmentation and analysis of early brain growth.** *Sci Rep* 2017;7:476 CrossRef Medline

26. Kainz B, Steinberger M, Wein W, et al. **Fast volume reconstruction from motion corrupted stacks of 2D slices.** *IEEE Trans Med Imaging* 2015;34:1901–13 CrossRef Medline

27. Priego G, Barrowman NJ, Hurteau-Miller J, et al. **Does 3T fetal MRI improve image resolution of normal brain structures between 20 and 24 weeks' gestational age?** *AJNR Am J Neuroradiol* 2017;38:1636–42 CrossRef Medline

28. Ortinau CM, Mangin-Heimos K, Moen J, et al. **Prenatal to postnatal trajectory of brain growth in complex congenital heart disease.** *Neuroimage Clin* 2018;20:913–22 CrossRef Medline

29. Chugani HT, Phelps ME, Mazziotta JC. **Positron emission tomography study of human brain functional development.** *Ann Neurol* 1987;22:487–97 CrossRef Medline

30. Boudes E, Gilbert G, Leppert IR, et al. **Measurement of brain perfusion in newborns: pulsed arterial spin labeling (PASL) versus pseudo-continuous arterial spin labeling (pCASL).** *Neuroimage Clin* 2014;6:126–33 CrossRef Medline

31. Im K, Grant PE. **Sulcal pits and patterns in developing human brains.** *Neuroimage* 2019;185:881–90 CrossRef Medline

32. Sun T, Hevner RF. **Growth and folding of the mammalian cerebral cortex: from molecules to malformations.** *Nat Rev Neurosci* 2014;15:217–32 CrossRef Medline